J Nondestruct Eval (2010) 29: 143–153
DOI 10.1007/s10921-010-0072-6

The Effect of Hardness on Eddy Current Residual Stress Profiling in Shot-Peened Nickel Alloys

Bassam A. Abu-Nabah · Waled T. Hassan · Daniel Ryan · Mark P. Blodgett · Peter B. Nagy

Published online: 22 June 2010

Abstract Recent research results indicate that eddy current conductivity measurements can be exploited for nondestructive evaluation of subsurface residual stresses in surface-treated nickel-base superalloy components. According to this approach, first the depth-dependent electric conductivity profile is calculated from the measured frequency-dependent apparent eddy current conductivity spectrum. Then, the residual stress depth profile is calculated from the conductivity profile based on the piezoresistivity coefficient of the material, which is determined separately from calibration measurements using known external applied stresses. This paper presents new results that indicate that in some popular nickel-base superalloys the relationship between the electric conductivity profile and the sought residual stress profile is more tenuous than previously thought. It is shown that in delta-processed IN718 the relationship is very sensitive to the state of precipitation hardening and, if left uncorrected, could render the eddy current technique unsuitable for residual stress profiling in components of 36 HRC or harder, i.e., in most critical engine applications. The presented experimental results show that the observed dramatic change in the eddy current response of hardened IN718 to surface treatment is caused by very fine nanometer-scale features of the microstructure, such as γ' and γ'' precipitates, rather than micrometer-scale features, such as changing grain size or δ phase and carbide precipitates.

Keywords Eddy current · Conductivity spectroscopy · Surface-treatment · Residual stress

B.A. Abu-Nabah
General Electric Aviation, Cincinnati, OH 45215, USA

W.T. Hassan
Rolls-Royce Corporation, Indianapolis, IN 46241, USA

D. Ryan
Honeywell Aerospace, Phoenix, AZ 85034, USA

M.P. Blodgett
Air Force Research Laboratory, WPAFB, Dayton, OH 45433, USA

P.B. Nagy (✉)
Department of Aerospace Engineering, University of Cincinnati, Cincinnati, OH 45221, USA
e-mail: peter.nagy@uc.edu

1 Introduction

Surface enhancement methods, such as shot peening (SP), laser shock peening (LSP), and low-plasticity burnishing (LPB), significantly improve the fatigue resistance and foreign object damage tolerance of metallic components by introducing beneficial near-surface compressive residual stresses. Moreover, the surface is slightly strengthened and hardened by the cold-working process. By far the most common way to produce protective surface layers of compressive residual stress is shot peening, though it is probably also the worst technique from the point of view of damaging cold work which substantially decreases the thermo-mechanical stability of the microstructure at elevated operating temperatures and leads to accelerated relaxation of the beneficial residual stresses [1]. Although LSP and LPB produce significantly deeper compressive residual stress than SP, their main advantage over SP is that they produce much less cold work on the order of 5–15% equivalent plastic strain.

Nondestructive residual stress assessment in surface-enhanced engine components is important because there is mounting evidence that it is not possible to reliably and accurately predict the remaining service life of such compo-

Report Documentation Page

Form Approved
OMB No. 0704-0188

1. REPORT DATE	2. REPORT TYPE	3. DATES COVERED
22 JUN 2010		**00-00-2010 to 00-00-2010**

4. TITLE AND SUBTITLE	5a. CONTRACT NUMBER
The Effect of Hardness on Eddy Current Residual Stress Profiling in Shot-Peened Nickel Alloys	5b. GRANT NUMBER
	5c. PROGRAM ELEMENT NUMBER
6. AUTHOR(S)	5d. PROJECT NUMBER
	5e. TASK NUMBER
	5f. WORK UNIT NUMBER
7. PERFORMING ORGANIZATION NAME(S) AND ADDRESS(ES) **General Electric Aviation,Cincinnati,OH,45215**	8. PERFORMING ORGANIZATION REPORT NUMBER
9. SPONSORING/MONITORING AGENCY NAME(S) AND ADDRESS(ES)	10. SPONSOR/MONITOR'S ACRONYM(S)
	11. SPONSOR/MONITOR'S REPORT NUMBER(S)

12. DISTRIBUTION/AVAILABILITY STATEMENT
Approved for public release; distribution unlimited

13. SUPPLEMENTARY NOTES

14. ABSTRACT

Recent research results indicate that eddy current conductivity measurements can be exploited for nondestructive evaluation of subsurface residual stresses in surfacetreated nickel-base superalloy components. According to this approach, first the depth-dependent electric conductivity profile is calculated from the measured frequency-dependent apparent eddy current conductivity spectrum. Then, the residual stress depth profile is calculated from the conductivity profile based on the piezoresistivity coefficient of the material, which is determined separately from calibration measurements using known external applied stresses. This paper presents new results that indicate that in some popular nickel-base superalloys the relationship between the electric conductivity profile and the sought residual stress profile is more tenuous than previously thought. It is shown that in delta-processed IN718 the relationship is very sensitive to the state of precipitation hardening and, if left uncorrected could render the eddy current technique unsuitable for residual stress profiling in components of 36 HRC or harder, i.e., in most critical engine applications. The presented experimental results show that the observed dramatic change in the eddy current response of hardened IN718 to surface treatment is caused by very fine nanometer-scale features of the microstructure, such as &#947 and &#947 precipitates, rather than micrometer-scale features, such as changing grain size or &#948 phase and carbide precipitates.

15. SUBJECT TERMS

16. SECURITY CLASSIFICATION OF:			17. LIMITATION OF ABSTRACT	18. NUMBER OF PAGES	19a. NAME OF RESPONSIBLE PERSON
a. REPORT	b. ABSTRACT	c. THIS PAGE			
unclassified	**unclassified**	**unclassified**	**Same as Report (SAR)**	**11**	

nents without properly accounting for the presence of near-surface compressive residual stresses [2]. Unfortunately, both the absolute level and spatial distribution of the residual stress are rather uncertain partly because the stress is highly susceptible to variations in the manufacturing process and partly because subsequently it tends to undergo thermo-mechanical relaxation at operating temperatures. The only currently available practical NDE method for residual stress assessment is based on X-ray diffraction (XRD) measurement that is limited to an extremely thin, less than 20 µm deep, surface layer [3]. Because of this limitation, XRD residual stress profiling necessitates the repeated removal of thin surface layers by electro-polishing, therefore the method is inherently destructive. When such layer removal is performed, the measured stress needs to be corrected for the stress relaxation and redistribution that occurs during layer removal [4].

2 Eddy Current Conductivity Spectroscopy

Because of the above discussed limitations, the NDE community has been looking for alternatives to characterize residual stress profiles in surface-treated engine components for many years and eddy current conductivity spectroscopy emerged as one of the leading candidates [5–27]. Eddy current residual stress profiling is based on the piezoresistivity of the material, i.e., on the characteristic dependence of the electric conductivity on stress. Figure 1 shows a schematic representation of physics-based eddy current residual stress profiling in surface-treated components. In order to remove the influence of the measurement system (coil size, shape, etc.) the actually measured complex electric impedance of the probe coil is first transformed into a so-called apparent eddy current conductivity (AECC) parameter. At a given inspection frequency, the AECC is defined as the electric conductivity of an equivalent homogeneous, non-magnetic, smooth, and flat specimen placed at a properly chosen distance from the coil that would produce the same complex electric coil impedance as the inhomogeneous specimen under study [15]. Near-surface residual stress assessment is based on the relative difference in electric conductivity between the compressed regions just below the surface and the intact material deep below the surface, where it is not affected by surface treatment. Accordingly, the apparent eddy current conductivity difference ΔAECC at each frequency is normalized to the AECC measured at the lowest available inspection frequencies.

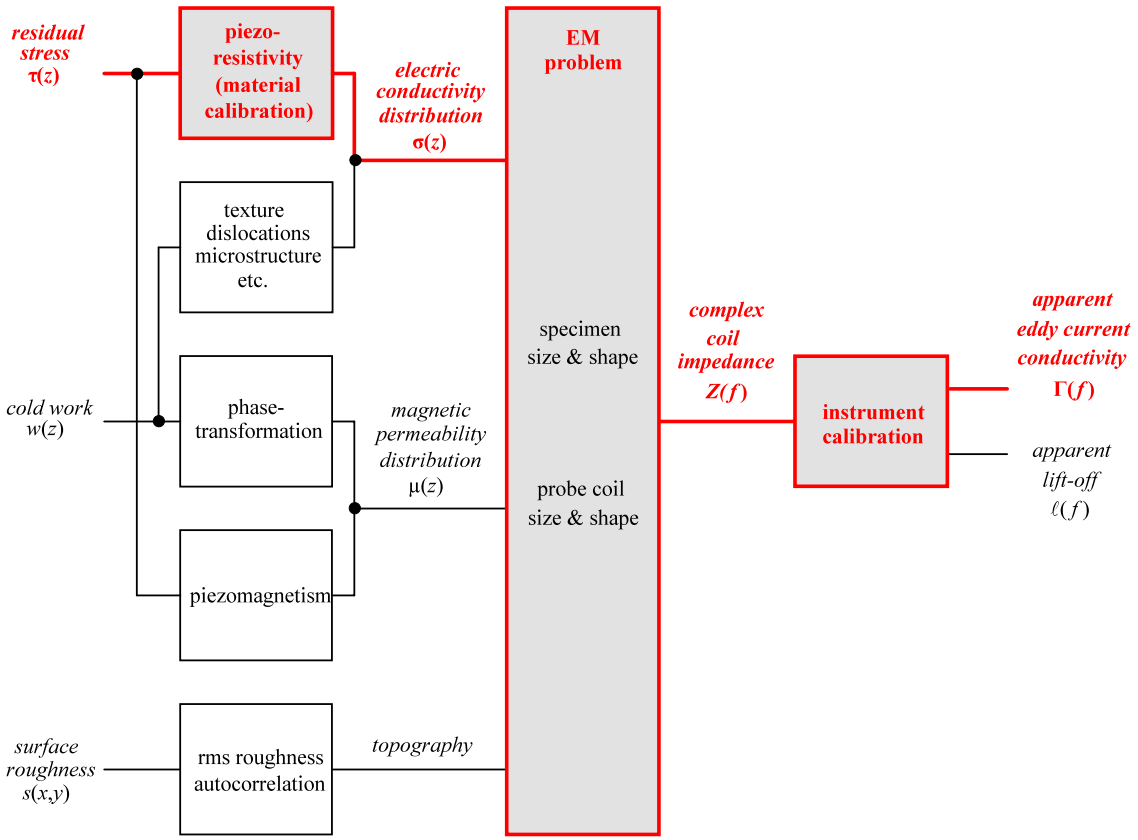

Fig. 1 A schematic representation of physics-based eddy current residual stress profiling in surface-treated components (the principal path is highlighted)

If spurious material (e.g., magnetic permeability) and geometric (e.g., surface roughness) variations can be neglected, the frequency-dependent AECC can be inverted for the depth-dependent electric conductivity profile (this principal path is highlighted in Fig. 1). Then, using the known piezoresistivity of the material, the sought residual stress profile can be calculated. Unfortunately, besides the sought near-surface residual stress, the measured complex electric coil impedance, and therefore also the inferred AECC, is also affected by the presence of cold work and surface roughness. The electric conductivity variation due to residual stress is usually weak (≈1%) and rather difficult to separate from these accompanying spurious effects. In certain materials, such as austenitic stainless steels, cold work might also cause significant magnetic permeability variation which affects the measured coil impedance. Fortunately, nickel-base superalloys do not exhibit such ferromagnetic transition from their paramagnetic state [19]. In addition, because of their significant hardness, shot-peened nickel-base superalloy components exhibit only rather limited surface roughness (≈2–3 μm rms), therefore the influence of geometrical irregularities is also limited. Still, as the inspection frequency increases the eddy current loop becomes squeezed closer to the rough surface, which creates a more tortuous, therefore longer, path and might lead to a perceivable drop of AECC above 30–40 MHz [28–30].

In order to translate the measured frequency-dependent AECC into a depth-dependent electric conductivity profile in a nonmagnetic medium, first a simplistic inversion technique was developed [16], which was recently followed by the development of a highly convergent iterative inversion technique [21]. Both techniques indicated that at any given frequency the measured AECC corresponds roughly to the actual electric conductivity at half of the standard penetration depth assuming that (i) the electric conductivity variation is limited to a shallow surface region of depth much less than the probe coil diameter, (ii) the relative change in electric conductivity is less than a few percents, and (iii) the electric conductivity depth profile is continuous and fairly smooth. Alternatively, best fitting of the measured electric coil impedance with the known analytical solution can be used assuming that the conductivity profile can be characterized by a small number of independent parameters [24]. Finally, the sought residual stress profile is calculated from the electric conductivity profile based on the piezoresistivity coefficient of the material, which is determined separately from material calibration measurements using known external applied stresses [17].

The main limitation of residual stress profiling by eddy current conductivity spectroscopy is that the feasibility of this technique seems to be limited to nickel-base superalloys, though some beneficial information on increasing hardness could be also obtained by this technique on titanium and aluminum alloys. Unfortunately, even in the case of nickel-base superalloys, there exist some serious limitations that adversely influence the applicability of the eddy current method. First, forged nickel-base superalloys often exhibit significant conductivity inhomogeneity that could interfere with subsurface residual stress characterization [18]. Second, these materials are susceptible to cold-work-induced microstructural changes that cause a conductivity increase similar or even larger than the primary conductivity increase caused by compressive residual stresses [19]. Third, the electrical conductivity in nickel-base superalloys is rather low (≈1.5% IACS) therefore the standard penetration depth is relatively high at a given inspection frequency (≈180 μm at 10 MHz). Therefore, we cannot fully reconstruct the critical near-surface part of the residual stress profile in moderately peened components using only typical inspection frequencies below 10 MHz. In such cases, special high-frequency inspection techniques are needed to extend the frequency range up to 50–80 MHz, i.e., beyond the range of commercially available instruments [22–26].

To illustrate the advantages of high-frequency conductivity spectroscopy, Fig. 2 shows the cold work (a) and residual stress (b) profiles obtained by destructive XRD measurements in shot-peened IN100 specimens of Almen 4A, 8A, and 12A peening intensities. For comparison purposes, Fig. 2(b) also shows the residual stress profiles reconstructed from the measured AECC spectra. Except for a sharper-than-expected near-surface "hook" observed in the Almen 8A specimen, which is most probably caused by imperfect lift-off rejection above 25 MHz, the general agreement between the AECC and XRD data is very good. In the first step, the depth-dependent electric conductivity change was calculated using the previously described iterative inversion procedure [21]. Then, the sought depth profile of the residual stress was estimated by neglecting cold work and surface roughness effects. In order to get the good overall agreement illustrated in Fig. 2(b), we had to use a corrected value of the electroelastic coefficient $\kappa_{ip} = -1.06$, which is 33% lower than the independently measured average value for IN100. The exact reason for the need for this "empirical" correction is currently not known, but it is likely connected to the issue of precipitation hardening discussed later in this paper and will require further investigation. However, it should be pointed out that this underestimation of the residual stress level by the inverted AECC relative to the destructive XRD results does not seem to be physically related to the experimentally observed overestimation in Waspaloy and IN718 alloys due to increasing electric conductivity caused by microstructural changes under extensive cold work [19]. Since a single correction factor was sufficient to bring all the AECC and XRD results into good agreement with each other for all three peening intensities in spite of

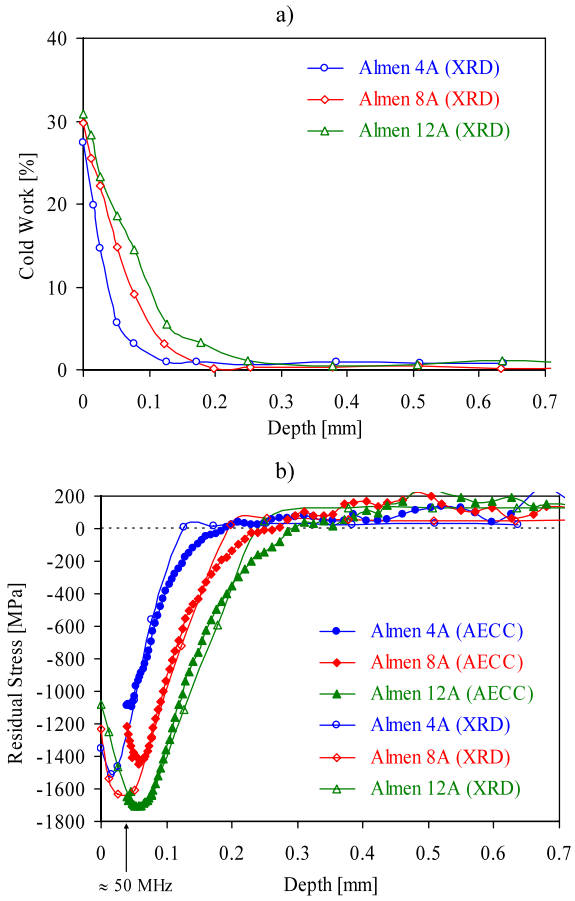

Fig. 2 XRD profiles of near-surface cold work (**a**) and residual stress (**b**) compared to the inverted eddy current residual stress profile in shot peened IN100 specimens of Almen 4A, 8A and 12A peening intensity levels

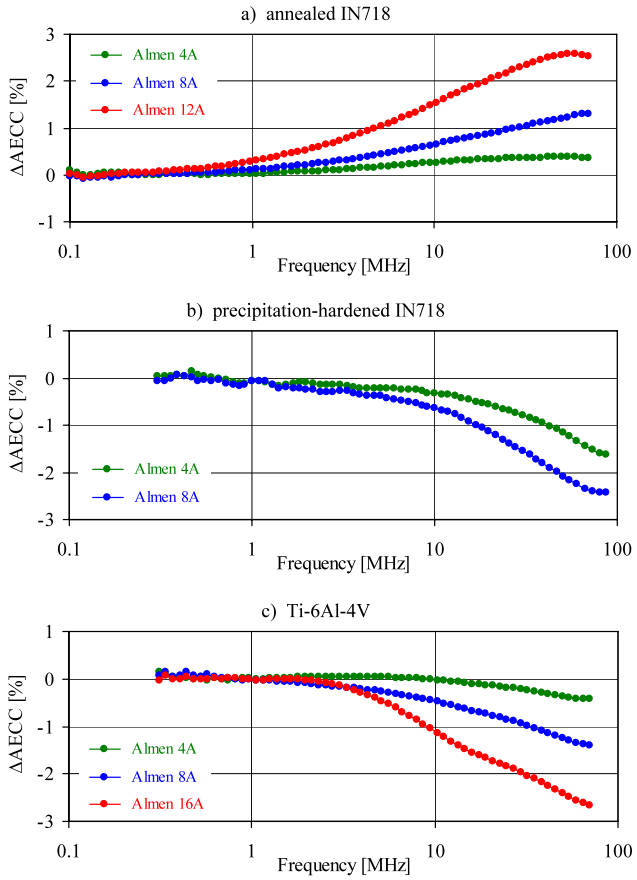

Fig. 3 Typical ΔAECC spectra measured in (**a**) annealed IN718, (**b**) precipitation-hardened IN718, and (**c**) Ti-6Al-4V specimens shot-peened to different intensities

their very different levels of cold work, the cause of this apparent underestimation by the AECC method is most probably the intrinsic variation of the electroelastic coefficient with microstructure.

Previous experimental observations indicated that the sensitivity of eddy current conductivity spectroscopy is fairly low, but still sufficient for residual stress profiling in certain surface-treated engine alloys. However, the electrical conductivity and its stress-dependence are rather sensitive to microstructural variations, therefore the selectivity of this method leaves much to be desired. Recent research revealed a series of situations where anomalous stress-dependence and relaxation behavior were observed [25, 26]. This is not surprising at all in the case of an inherently indirect nondestructive method and should not lead to abandoning the eddy current approach, especially since no better alternative is known at this point. A recent paper by the authors reviewed four previously unreported experimental observations of anomalous materials behavior and proposed further research efforts to better understand the underlying physical mechanisms and to mitigate the adverse influence of these phenomena on eddy current residual stress profiling [25]. The most important case of apparently anomalous behavior was observed in precipitation-hardened IN718 material that is very different from those of the commercial versions reported in the literature [15, 18–24].

Figure 3 shows typical AECC spectra measured in (a) annealed IN718, (b) precipitation-hardened IN718, and (c) Ti-6Al-4V specimens shot-peened to different intensities. Annealed IN718 shown in Fig. 3(a) exhibits the classical behavior of materials with negative electroelastic coefficient, i.e., the AECC change caused by compressive subsurface stresses is positive and increases with peening intensity as well as with inspection frequency. It has been shown that in such soft (HRC 24) materials the AECC change monotonically decreases with thermal relaxation [15]. In contrast, precipitation-hardened IN718 shown in Fig. 3(b) exhibits opposite behavior with apparently positive electroelastic coefficient, i.e., the measured AECC change is negative and increases with peening intensity as well as with inspection frequency [25, 26], therefore it is similar to the behavior observed in Ti-6Al-4V shown in Fig. 3(c), which is dominated by cold work effects [31].

One obvious indication of the different microstructure of annealed and precipitation-hardened IN718 is that the electric conductivity is perceivably lower in the annealed material (≈1.5% IACS) than in the hardened one (≈1.63% IACS). It could be expected that the electroelastic coefficient also changes, at least slightly, with hardness. Unfortunately, the specimens used in this study did not have the bar-shape geometry that would have allowed us to measure their electroelastic coefficients by the standard method developed for this purpose [17]. Therefore, we had to rely on electroelastic coefficient measurements on similarly processed and hardened IN718 specimens from an earlier study and it is left for a follow-up study to establish whether the electroelastic coefficient exhibits a perceivable dependence on precipitation hardening. Our earlier quasi-static materials calibration measurements showed that the unitless normalized electroelastic coefficient of the fully hardened (HRC 46) material is about $\kappa_{ip} = -1.14$, i.e., also negative, though its magnitude is roughly 30% smaller than that of the corresponding value ($\kappa_{ip} = -1.57$) found in annealed IN718 [25]. In other words, the precipitation-hardened material exhibits a markedly different behavior from the annealed version. The same behavior was reported by Hillman et al. who also discovered that in the hardened alloy thermal relaxation produces an increase rather than decrease in the magnitude of the AECC change [26].

Hillman et al. suggested that "macroscopic" features of the microstructure, such as reduced grain size and increased concentration of coarse (≈1-μm-diameter) carbide particles, might be responsible for the observed differences in eddy current behavior between different states of microstructures created by very different thermal processing [26]. The main goal of our current research effort was to verify whether this is indeed the case or the higher electric conductivity and, most importantly, the negative ΔAECC spectrum in surface-treated components are actually due to much more subtle "microscopic" features of the microstructure, e.g., the changing volume fraction of very fine γ' and γ'' precipitates that are far too small (≈10-nm-diameter) to observe on low-magnification micrographs.

3 Influence of Precipitation Hardening

In order to further investigate the influence of precipitation hardening on eddy current residual stress profiling in surface-treated nickel alloys, a series of fine-grain δ-processed IN718 specimens were provided by Honeywell Engines of Phoenix, Arizona. δ-processing of IN718 uses an intentional δ phase precipitation cycle and subsequent thermomechanical processing to produce uniform fine grain distribution [32, 33]. Table 1 lists the thermal treatment times and resulting hardness levels of twelve specimens used in our tests. First, all twelve specimens were solution annealed at 982°C for 30 minutes and then air fan cooled to room temperature. Then specimens #3 through #10 were partially aged by heating the specimens to 704°C and holding them for the listed treatment time before air fan cooling to room temperature. Samples #11 and #12 were exposed to the full two-step aging thermal cycle (704°C—8 hrs, 649°F—8 hrs). At each treatment time two specimens were produced, therefore there were only six different treatment levels with the small random difference between two specimens of the same treatment level indicating the repeatability of the treatment. After heat treatment, all twelve specimens were machined into 25.4 mm × 25.4 mm × 12.5 mm rectangular blocks and then shot peened to Almen 4A intensity on one side and to Almen 6A intensity on the other side.

Figure 4 shows the optical images of the δ-processed microstructure in IN718 specimens that represent the six different hardness levels achieved by the six different treatment

Table 1 Heat treatment procedures and Rockwell C hardness levels of twelve fine-grain IN718 specimens used in our tests

ID	Solution anneal at 982°C	Aging at 704°C	Post aging at 649°C	HRC
#1	30 minutes	none	none	24.9
#2	30 minutes	none	none	26.5
#3	30 minutes	0.1 minutes	0 hours	31.0
#4	30 minutes	0.1 minutes	0 hours	33.8
#5	30 minutes	6 minutes	0 hours	31.9
#6	30 minutes	6 minutes	0 hours	33.8
#7	30 minutes	24 minutes	0 hours	35.9
#8	30 minutes	24 minutes	0 hours	35.7
#9	30 minutes	2 hours	0 hours	39.0
#10	30 minutes	2 hours	0 hours	39.3
#11	30 minutes	8 hours	8 hours	45.5
#12	30 minutes	8 hours	8 hours	45.3

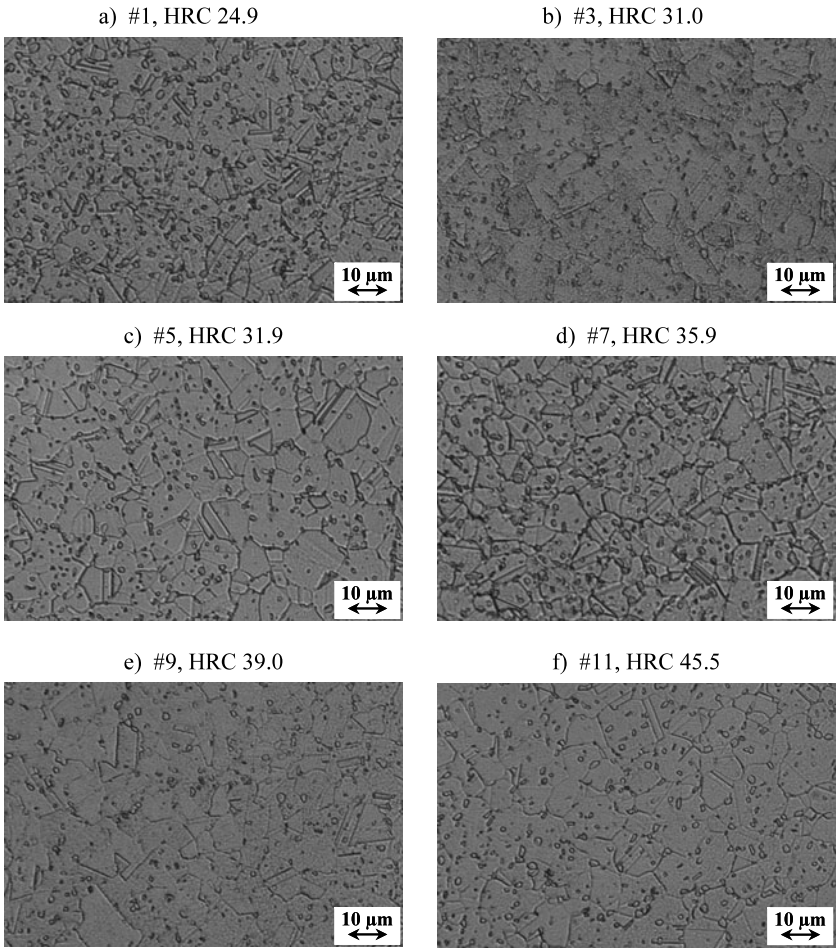

Fig. 4 Optical images of the microstructure in δ-processed IN718 specimens of various hardness levels. The average grain size is approximately 10 µm while the average δ phase and carbide precipitate size is 1–2 µm

times listed in Table 1. Most of the visible particles are δ precipitates rather than carbides which are concentrated at the grain boundaries. The average grain size remained constant at approximately 10 µm in all specimens. Similarly, the average δ precipitate and carbide particle size also remained constant at around 1–2 µm and their number density did not change perceivably either. Therefore, we can conclude that any change in hardness and eddy current response exhibited by these specimens must be due mainly to more subtle changes in the density and size of fine precipitates that are not visible on these low-magnification micrographs. It is known that strengthening of IN718 is mainly caused by γ'' precipitates and, to a much lesser degree, by γ' precipitates (γ'' precipitates are disk-shaped Ni_3Nb particles with body-centered tetragonal (bct) structure while γ' precipitates are spherical $Ni_3(Al, Ti)$ particles of cubic structure).

Figure 5 shows superlattice dark-field TEM images of the microstructure in IN718 specimens of various hardness levels. These images were produced by combining the (001) and (011) γ'' diffraction peaks, therefore the bright specks are very fine γ'' precipitates that play crucial roles in both hardening the material and controlling its electric properties. Figure 5 illustrates that thermal aging causes coarsening of the γ'' precipitates. The coarsening of γ'' precipitates follows the Lifshitz–Slyozov–Wagner (LSW) time-law [34, 35] according to which the average volume of γ'' precipitates grows linearly with aging time

$$L^3 - L_0^3 \approx K''(T)t, \tag{1}$$

where L is the mean-diameter of the disk-shaped γ'' precipitates, L_0 is the initial diameter before thermal aging, t is the aging time, and K'' is an empirical constant determined by the aging temperature T (a similar relationship exists for γ' precipitates as well). At 704°C, the range of K'' values in the literature is 0.08–0.3 nm^3/s for mean-diameters between 10 and 50 nm [36–38].

The intrinsic and extrinsic factors that affect the electrical conductivity of nickel-base alloys are likely to be complex and depend on the nature of both the γ matrix (composition, presence of short-range order, etc.) and γ' and γ'' precipitates (size, volume fraction) as well as on how each constituent is affected by cold work. In general, solute atoms in solid solution decrease the electric conductivity by reducing the strict periodicity of the lattice and thereby increasing electron scattering, as does cold working to a

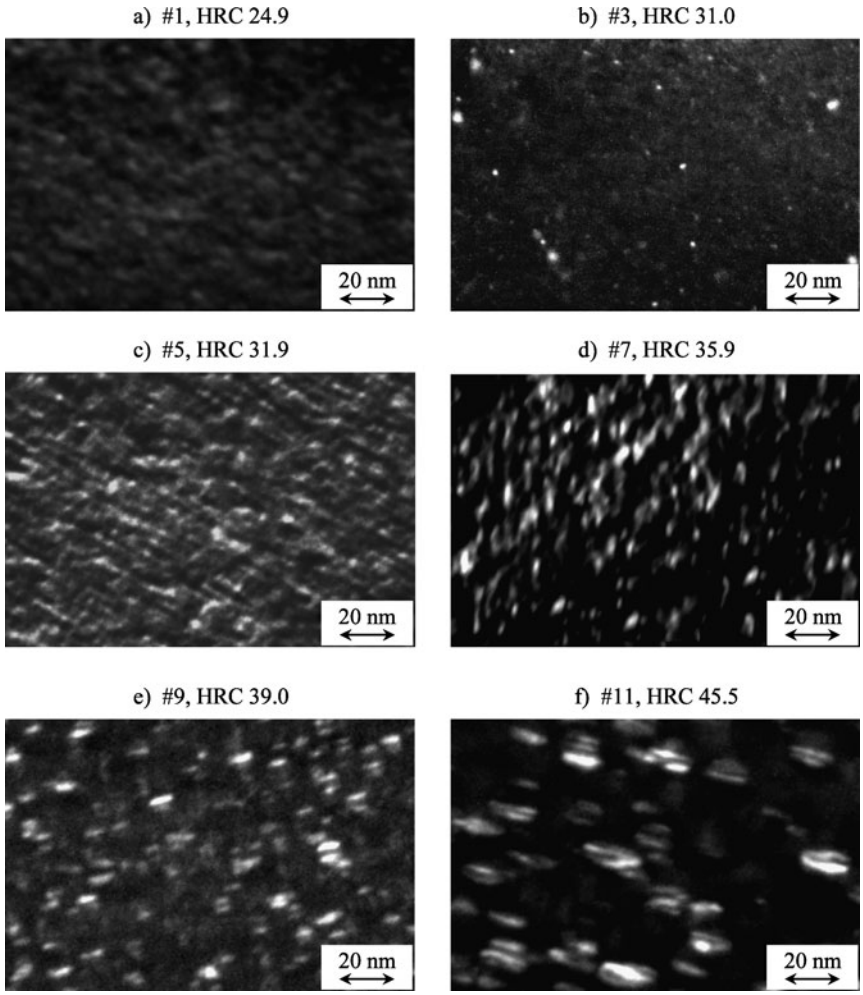

Fig. 5 Superlattice dark-field TEM images of the microstructure in IN718 specimens of various hardness levels

smaller extent by producing an increasing density of defects (dislocations, vacancies, etc.). On the other hand, precipitation of ordered phases generally increases conductivity by decreasing the solute concentration and hence scattering from the solid solution matrix in which they form. Our current study is limited to establishing the crucial role of γ'' precipitate coarsening in the eddy current response of precipitation-hardened IN718 nickel-base superalloy. The underlying physical mechanisms responsible for this behavior will have to be the subject of future investigations.

Figure 6 shows the XRD residual stress and cold work profiles of six IN718 specimens listed in Table 1 after shot peening. According to Figs. 6(a) and 6(b), the average peak (compressive) stress at the surface was -1270 MPa and -1324 MPa for the six surfaces of Almen 4A and Almen 6A peening intensity, respectively. A more significant change can be observed by comparing the half-peak depth of the compressed surface layers, which increased from ≈ 0.05 mm at Almen 4A intensity to ≈ 0.076 mm at Almen 6A intensity. More importantly, the residual stress profiles do not exhibit any perceivable trend with increasing hardness, i.e., within experimental uncertainties, they are all the same regardless of the level of hardening. A similar conclusion can be drawn by comparing the XRD cold-work profiles shown in Figs. 6(b) and 6(d). For simplicity, the figures show the width of the observed XRD peak, which is directly related to the equivalent plastic strain in the material. As expected, the average peak widening, therefore also the average cold work, is somewhat higher at the higher peening intensity level, but, even in this un-calibrated form, the XRD data clearly indicates that the changing hardness level did not significantly affect the cold work profiles. In summary, the presented metallographic and XRD results suggest that any change in the AECC spectra of these shot-peened specimens with increasing hardness must be mainly due to the strong influence of very fine γ'' precipitates on how the eddy current conductivity spectrum of the material responds to shot peening.

Figure 7 shows the bulk AECC versus Rockwell C hardness in the twelve shot-peened IN718 specimens listed in Table 1. The error bars represent the estimated $\pm 1\%$ uncertainty of the absolute AECC measurement and the solid lines are quadratic regressions. Since we did not have a chance to measure the electric conductivity of the intact specimens be-

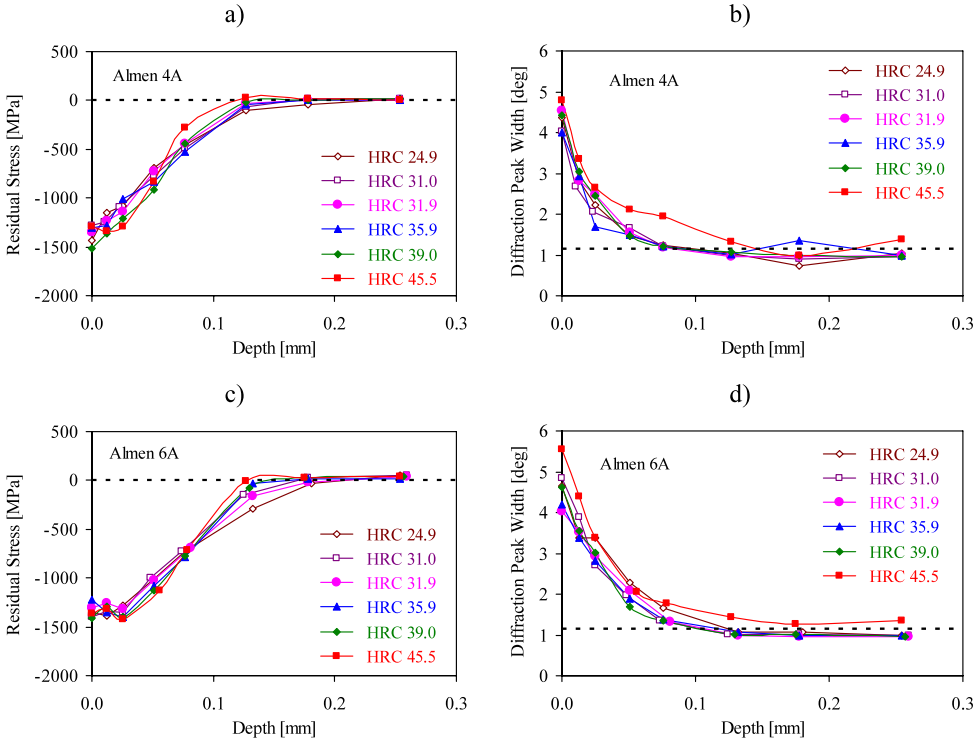

Fig. 6 XRD residual stress and cold work profiles of shot-peened IN718 specimens of various hardness levels

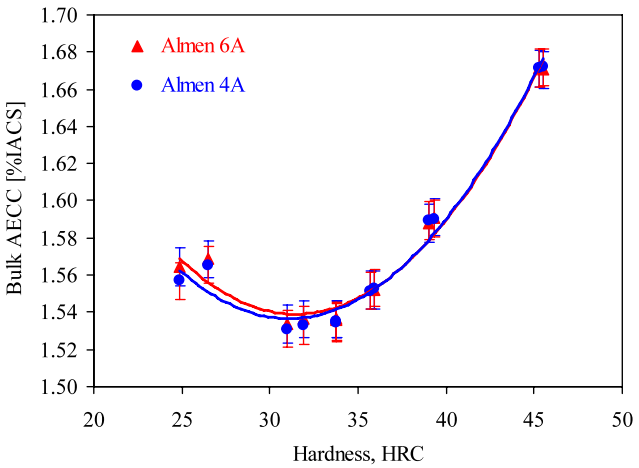

Fig. 7 Bulk AECC versus Rockwell C hardness in shot-peened IN718 specimens

fore shot peening, we defined the intact "bulk" AECC as the average AECC measured between 0.6 and 1.1 MHz, a frequency range that corresponds to a depth range of roughly 0.26–0.36 mm. As expected, this bulk parameter is very susceptible to precipitation hardening, but not affected at all by surface treatment. A quick comparison with the residual stress and cold work profiles shown in Fig. 6 verifies that at such depths the effects of shot peening are completely negligible. An additional proof of this fact is provided by Fig. 7 which shows that the bulk electric conductivity is essentially the same at both peening intensities regardless of the hardness level. As the hardness increases, the electric conductivity first drops from ≈1.56% IACS at HRC 25 to ≈1.54% IACS at HRC 32, then increases to ≈1.67% IACS at HRC 46. It is important to point out that over the hardness range of practical interest for engine applications (above HRC 40) the electric conductivity is a monotonic, therefore invertible, function of hardness, which could be exploited later to correct for the spurious influence of hardness on our eddy current results.

Figure 8 shows the apparent eddy current conductivity change ΔAECC spectra in twelve shot-peened specimens of Almen 4A and 6A intensity. At around HRC 39 the "classical" positive ΔAECC changes sign, while above HRC 43 the negative ΔAECC is small but measurable. The continuous transformation of the regular positive ΔAECC spectrum into an irregular negative ΔAECC spectrum as the hardness increases indicates the increasing role of spurious cold work effects over the principal residual stress effect. The gradual transformation of the ΔAECC spectrum of shot-peened IN718 clearly indicates a close correlation with the gradual growth of γ'' precipitates, although at this point the contribution of other subtle changes, such as short-range ordering in the γ matrix, cannot be excluded either. Undoubtedly, this indirect influence of hardness on the eddy current response of surface-treated nickel alloys presents a formidable problem for physics-based residual stress profiling, but does not exclude the feasibility of a simpler empirical method since the bulk conductivity of the material can be exploited for correction purposes as a measure of precipitation hardening.

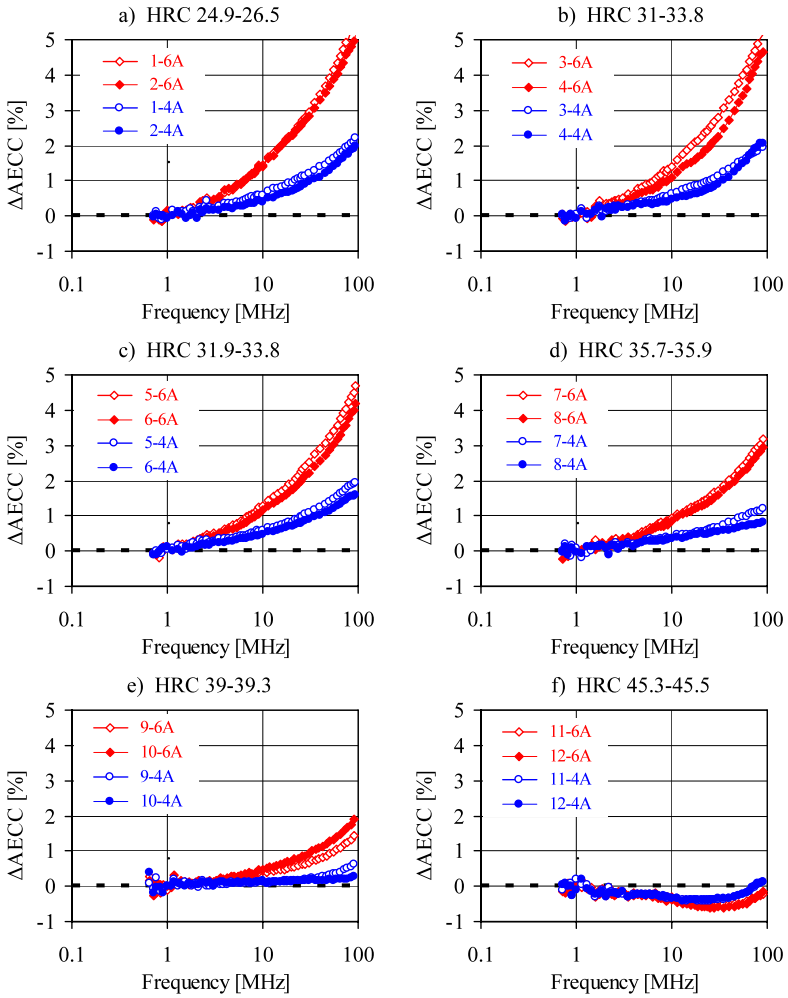

Fig. 8 Apparent eddy current conductivity change (ΔAECC) spectra in twelve shot-peened specimens of Almen 4A and 6A intensity

4 Conclusions

The potential of thermal relaxation in shot-peened engine components at elevated operational temperatures necessitates repeated checks of the remaining residual stress levels during periodic maintenance. Since existing inspection methods either cannot be applied to subsurface residual stress assessment or are destructive in nature, new nondestructive characterization methods are being sought to replace or supplement them. Eddy current conductivity spectroscopy has emerged as one of the leading candidates for nondestructive residual stress profiling in surface-treated metals. This is an experimental method that will require further research before it can be applied in field inspection. Currently, its feasibility for quality monitoring during manufacturing and assessing subsequent relaxation during service has been demonstrated only for certain nickel-base superalloys. The main limitation of residual stress profiling by eddy current conductivity spectroscopy is that, although the method is sensitive enough to weak elastic strains to be practically useful, it is not sufficiently selective to them. Because of these limitations, eddy current conductivity spectroscopy cannot be expected to replace XRD residual stress measurements. However, because of its relative simplicity and nondestructive nature, it might supplement the more accurate but destructive XRD technique.

This paper presented new experimental results that indicate that in some popular nickel-base superalloys the relationship between the electric conductivity depth profile and the sought residual stress profile is more tenuous than previously thought. It was shown that in IN718 the relationship is very sensitive to the state of precipitation hardening and, if left uncorrected, could render this technique unsuitable for eddy current residual stress profiling in components of 36 HRC or harder, i.e., in most critical engine applications. The presented experimental results suggest that the observed dramatic change in the eddy current response of the material to surface treatment in hardened IN718 is probably caused by very fine nanometer-scale γ'' and, to a much less degree, γ' precipitates rather than micrometer-scale features, such as changing grain size and δ phase and carbide precipitates. This study was limited to establishing the crucial role

of γ'' precipitate coarsening in eddy current characterization of surface-treated precipitation-hardened IN718 nickel-base superalloys. The underlying physical mechanisms responsible for this behavior will have to be further investigated in the future.

Finally, it should be stated that, in theory, differences in processing of IN718 might be important for the questions under investigation because the δ and γ'' phases have the same chemical composition, therefore precipitation of δ phase consumes some of the Nb that is available for the formation of γ'' precipitates during hardening by thermal aging. Although our present study used exclusively delta-processed IN718, a preliminary study [26] conducted at the Fraunhofer Institute in Germany showed that a very similar switch in the sign of the apparent eddy current conductivity change (ΔAECC) caused by shot peening with increasing hardness also occurs in regularly processed IN718. A similar systematic study on regular IN718 is currently underway in collaboration with UES and AFRL RXLP and the results of that study will be reported in the near future.

Acknowledgements This work was supported by the Metals Affordability Initiative (MAI) Consortium under USAF/AFMC Technology Investment Agreement FA8650-06-2-5211 and MAI Agreement FA8650-07-2-5242 with Tom Johnson of Honeywell acting as the Program Manager. The diffraction measurements reported in this study were made by Lambda Research of Cincinnati, Ohio. The TEM images were provided by Professor Vijay Vasudevan of the University of Cincinnati. The authors would like to acknowledge valuable discussions and ongoing collaboration with Susanne Hillmann and Norbert Meyendorf of the Fraunhofer Institute for NDT in Dresden, Germany, and Joachim Bamberg and Hans-Uwe Baron of MTU Aero Engines of Munich, Germany.

References

1. Prevéy, P.S.: The effect of cold work on the thermal stability of residual compression in surface enhanced IN718. In: Proceedings of 20th ASM Materials Solutions Conference, pp. 426–434. ASM International, Materials Park (2001)
2. Withers, P.J.: Residual stress and its role in failure. Rep. Prog. Phys. **70**, 2211 (2007)
3. Hauk, V.: Structural and Residual Stress Analysis by Nondestructive Methods, pp. 3–16. Elsevier, Amsterdam (1997)
4. Moore, M.G., Evans, W.P.: Mathematical correction for stress in removed layers in X-ray diffraction residual stress analysis. SAE Trans. **66**, 340 (1958)
5. Goldfine, N.: Real-time, quantitative materials characterization using quasistatic spatial mode sensing. In: 41st Army Sagamore Conference, August, 1994
6. Goldfine, N., Clark, D., Lovett, T.: Materials characterization using model based meandering winding eddy current testing (MWET). In: EPRI Topical Workshop: Electromagnetic NDE Applications in the Electric Power Industry, Charlotte, NC, August 21–23, 1995
7. Schoenig, F.C. Jr., Soules, J.A., Chang, H., DiCillo, J.J.: Eddy current measurement of residual stresses induced by shot peening in titanium Ti-6Al-4V. Mater. Eval. **53**, 22 (1995)
8. Blaszkiewicz, M., Albertin, L., Junker, W.: The eddy current technique for determining residual stresses in steels. Mater. Sci. Forum **210**, 179 (1996)
9. Goldfine, N., Clark, D.: Near surface material property profiling for determination of SCC susceptibility. In: EPRI Balance-of Plant Heat Exchanger NDE Symposium, Jackson, WY, June 10–12, 1996
10. Chang, H., Schoenig, F.C. Jr., Soules, J.A.: Eddy current offers a powerful tool for investigation of residual stress and other metallurgical properties. Mater. Eval. **57**, 1257 (1999)
11. Lavrentyev, A.I., Stucky, P.A., Veronesi, W.A.: Feasibility of ultrasonic and eddy current methods for measurement of residual stress in shot peened metals. In: Review of Progress in QNDE, vol. 19, pp. 1621–1628. AIP, Melville (2000)
12. Fisher, J.M., Goldfine, N., Zilberstein, V.: Cold work quality assessment and fatigue characterization using conformable MWM™eddy current sensors. In: 49th Defense Working Group on NDT, October 31–November 2, 2000
13. Zilberstein, V., Sheiretov, Y., Washabaugh, A., Chen, Y., Goldfine, N.J.: Applications of spatially periodic field eddy current sensors for surface layer characterization in metallic alloys. In: Review of Progress in QNDE, vol. 20, pp. 985–995. AIP, Melville (2001)
14. Zilberstein, V., Fisher, M., Grundy, D., Schlicker, D., Tsukernik, V., Vengrinovich, V., Goldfine, N., Yentzer, T.: Residual and applied stress estimation from directional magnetic permeability measurements with MWM sensors. ASME J. Press. Vessel Technol. **124**, 375 (2002)
15. Blodgett, M.P., Nagy, P.B.: Eddy current assessment of near-surface residual stress in shot-peened nickel-base superalloys. J. Nondestruct. Eval. **23**, 107 (2004)
16. Yu, F., Nagy, P.B.: Simple analytical approximations for eddy current profiling of the near-surface residual stress in shot-peened metals. J. Appl. Phys. **96**, 1257 (2004)
17. Yu, F., Nagy, P.B.: Dynamic piezoresistivity calibration for eddy current nondestructive residual stress measurements. J. Nondestruct. Eval. **24**, 143 (2005)
18. Yu, F., Blodgett, M.P., Nagy, P.B.: Eddy current assessment of near-surface residual stress in shot-peened inhomogeneous nickel-base superalloys. J. Nondestruct. Eval. **25**, 17 (2006)
19. Yu, F., Nagy, P.B.: On the influence of cold work on eddy current characterization of near-surface residual stress in shot-peened nickel-base superalloys. J. Nondestruct. Eval. **25**, 107 (2006)
20. Nakagawa, N., Lee, C., Shen, Y.: A high-frequency eddy current inspection system and its application to the residual stress characterization. In: Review of Progress in QNDE, vol. 25, pp. 1418–1425. AIP, New York (2006)
21. Abu-Nabah, B.A., Nagy, P.B.: Iterative inversion method for eddy current profiling of near-surface residual stress in surface-treated metals. NDT&E Int. **39**, 641 (2006)
22. Abu-Nabah, B.A., Nagy, P.B.: High-frequency eddy current conductivity spectroscopy for residual stress profiling in surface-treated nickel-base superalloys. NDT&E Int. **40**, 405 (2007)
23. Abu-Nabah, B.A., Nagy, P.B.: Lift-off effect in high-frequency eddy current conductivity spectroscopy. NDT&E Int. **40**, 555 (2007)
24. Shen, Y., Lee, C., Lo, C.C.H., Nakagawa, N., Frishman, A.M.: Conductivity profile determination by eddy current for shot-peened superalloy surfaces toward residual stress assessment. J. Appl. Phys. **101**, 014907 (2007)
25. Abu-Nabah, B.A., Yu, F., Hassan, W.T., Blodgett, M.P., Nagy, P.B.: Eddy current residual stress profiling in surface-treated engine alloys. Nondestr. Test. Eval. **24**, 209 (2009)
26. Hillmann, S., Heuer, H., Baron, H.U., Bamberg, J., Yashan, A., Meyendorf, N.: Near-surface residual stress profiling with high frequency eddy current conductivity measurement. In: Review of Progress in QNDE, vol. 28, pp. 1349–1355. AIP, New York (2009)

27. Sekine, Y., Soyama, H.: Evaluation of the surface of alloy tool steel treated by cavitation shotless peening using an eddy current method. Surf. Coat. Technol. **203**, 2254 (2009)
28. Blodgett, M.P., Ukpabi, C.V., Nagy, P.B.: Surface roughness influence on eddy current electrical conductivity measurements. Mater. Eval. **61**, 765 (2003)
29. Kalyanasundaram, K., Nagy, P.B.: A simple numerical model for calculating the apparent loss of eddy current conductivity due to surface roughness. NDT&E Int. **37**, 47 (2004)
30. Yu, F., Nagy, P.B.: Numerical method for calculating the apparent eddy current conductivity loss on randomly rough surfaces. J. Appl. Phys. **95**, 8340 (2004)
31. Abu-Nabah, B., Nagy, P.B.: The feasibility of eddy current conductivity spectroscopy for near-surface cold work profiling in titanium alloys. In: Review of Progress in QNDE, vol. 27, pp. 1228–1235. AIP, New York (2008)
32. Ruiz, C., Obabueki, A., Gillespie, K.: Evaluation of the microstructure and mechanical properties of delta processed alloy 718. In: Superalloys 1992, pp. 33–42. Minerals Met. & Mat. Soc., Warrendale (1992)
33. Zhang, H.Y., Zhang, S.H., Cheng, M., Li, Z.X.: Deformation characteristics of δ phase in the delta-processed Inconel 718 alloy. Mater. Charact. **61**, 49 (2010)
34. Lifshitz, I.M., Slyozov, V.V.: The kinetics of precipitation from supersaturated solid solutions. J. Phys. Chem. Solids **19**, 35 (1961)
35. Wagner, C.: Theory of aging by precipitation coarsening. Z. Elektrochem. **65**, 581 (1961)
36. Devaux, A., Nazé, L., Molins, R., Pineau, A., Organista, A., Guédou, J.Y., Uginet, J.F., Héritier, P.: Gamma double prime precipitation kinetic in Alloy 718. Mater. Sci. Eng. A **486**, 117 (2008)
37. Han, Y.F., Deb, P., Chaturvedi, M.C.: Coarsening behaviour of γ''- and γ'-particles in Inconel alloy 718. Met. Sci. **16**, 555 (1982)
38. Sundaraman, M., Mukhopadhyay, P., Banerjee, S.: Some aspects of the precipitation of metastable intermetallic phases in Inconel 718. Metall. Mater. Trans. A **23**, 2015 (1992)